Semi-rigid biopolyurethane foams based on palm-oil polyol and reinforced with cellulose nanocrystals

Xiaojian Zhou[a], Mohini M Sain[a,b], Kristiina Oksman [a,b*]

[a] *Division of Materials Science, Composite Centre Sweden,*

Luleå University of Technology, 971 87 Luleå, Sweden

[b] *Centre for Biocomposite and Biomaterials Processing, Faculty of Forestry,*

University of Toronto, 33 Willcocks Street, Toronto, Canada M5S 3B3

Abstract

In this study, water-blown biopolyurethane (BPU) foams based on palm oil were developed and cellulose nanocrystals (CNC) were incorporated to improve the mechanical properties of the foams. In addition, the foams were compared with petroleum polyurethane (PPU) foam. The foam properties and cellular morphology were characterized. The obtained results revealed that a low-density, semi-rigid BPU foam was prepared using a new formulation. CNC as an additive significantly improved the compressive strength from 54 to 117 kPa. Additionally, cyclic compression tests indicated that the addition of CNC increased the rigidity, leading to decreased deformation resilience. The dimensional stability of BPU foams was increased with increasing CNC concentration for both heating and freezing conditions. Therefore, the developed BPU nanocomposite foams are expected to have great potential as core material in composite sandwich panels as well as in other construction materials.

Key words: A. Foams; A. Nano-structures; B. Physical properties; B. Microstructure

Corresponding author Kristiina Oksman Tel.:+46 920 49 33 71

E-mail address: kristiina.oksman@ltu.se

1. Introduction

Polyurethane (PU) foams as core material for sandwich composite laminates have been widely used in many applications due to their mechanical properties, light weight, versatility and insulation performance [1]. PU foams are usually prepared by the reaction of petroleum-based polyol with isocyanate. In general, catalysts, surfactants and blowing agents are employed to regulate the properties and the cell morphology. Commercial isocyanates and polyols for PU foam preparation are derived from petroleum, which is expensive and toxic, and are based on non-renewable resources. From the used raw materials, up to now, only the polyol can be partially replaced or even fully replaced using bio-polyols, especially starch polyols, sugar polyols, natural oil polyols or liquefaction products [2-5].

The most promising commercial bio-polyols used for PU foam preparation are natural oil polyols, such as soybean oil polyol [6,7], castor oil polyol [8] and palm oil polyol [9-11]. These materials are not only abundant and renewable resources, but are also easily chemically modified, resulting in excellent properties and relatively low cost [12,13]. There is, however, one distinct drawback with bio-polyols for foam preparation and that is that their low mechanical strength, cannot meet the demands of specific applications [7]. As composites are being used in an increasing number of applications, improvement in the mechanical properties is of interest. Consequently, there has been a growing interest in wood waste, clays, cellulose nanocrystals and nanofibers, nanochitin and cellulose-fiber-reinforced PU foams [14-24]. It was found that the mechanical strength and Young's modulus can be significantly improved, cell morphology and cell size distributions were optimized, and thermal behavior was influenced using very low amounts of these additives and reinforcements.

Cellulose nanocrystals (CNC) have a high surface area, high aspect (length/diameter) ratio, unique morphology, low density, high specific strength and modulus, and low coefficient of thermal expansion. Owing to these features, cellulose nanocrystals have attracted great interest during recent years [21, 24-30]. Up to 10% of CNC addition in reinforced polyol-based polyurethane foams was studied by Li et al. [21]. Only few publications are found regarding the effect of nanocellulose as reinforcement for bio-polyol based PU foams, especially with regard to bio-polyol with very low hydroxyl value and functionality for PU foam preparation [19, 31].

In this study, water-blown semi-rigid BPU foams were developed using a foaming formulation in the presence of a blowing agent, catalysts and surfactants. The influence of CNC on the foam performance was investigated using scanning electron microscopy (SEM), universal compression testing and thermogravimetric analysis (TGA). A standard petroleum polyol PU foam was prepared and used as a reference foam.

2. Materials and methods

2.1. Materials

Palm oil polyol (Polygreen 3110) with hydroxyl value of 98 mg KOH/g, viscosity of 1660 mPas, functionality of 2 and acid number of 1.37 mg KOH/g was supplied by PolyGreen, Malaysia, and used as polyol for BPU foam preparation. Petroleum polol (Polyol 3165) with a hydroxyl value of 165 mg KOH/g, viscosity of 350 mPas and functionality of 3 was supplied by Perstorp, Sweden, for PPU foam preparation.

Commercial pMDI (polymeric methane diphenyl isocyanate) (ISO pMDI 92140) with –NCO content of 31%, viscosity of 250 mPas and functionality of 2.7 was purchased from Lagotech AB, Sweden.

Freeze-dried cellulose nanocrystals (2012-FPL-CNC-043) hydrolyzed from cellulose pulp were supplied by USDA Forest Service, Madison, USA.

Laboratory-grade chemical agents such as catalysts (triethylamine and dibutyltin dilaurate) and surfactants (polydimethyl siloxane and silicone oil) were obtained from VWR and Sigma Aldrich, Germany. Distilled water was used as blowing agent.

2.2. Foaming process

The foams were prepared according to the process presented in Fig. 1. First, the polyol and the CNC were mixed for 2 min under mechanical stirring in a plastic beaker. When the mixture became homogeneous, catalysts and surfactants were added and mixed for 30 s, and then pMDI was added and vigorously stirred for 20 s. The blowing agent (water) was added in the last step, and mixed for 10 s with the same stirring speed, and then the foaming began after a short time. Finally, white, semi-rigid foam was obtained within a few seconds. Neat polyurethane foams were prepared using a similar foaming process in the absence of CNC. The foam was removed from the foaming beaker after 1 h and allowed to post-cure at room temperature for 1 week prior the characterization.

The formulations used are shown in Table 1 and to ensure the index for the foam formulation was maintained at 1.5, 126 and 150 phr of pMDI was used for BPU and PPU respectively. In the formulation it is assumed that the water, added as blowing agent, will also react with pMDI and thus is included in the calculation of the -NCO/-OH index. BPU foams are based on the bio-polyol with pMDI and PPU foams are based on the petroleum polyol with pMDI. The parts of each component are based on per hundred parts of the polyol, designated as phr. Thus, BPU0, BPU1, BPU2, BPU4 and BPU8 are referred to as 0, 1, 2, 4 and 8 phr of CNC.

Foams were characterized in terms of foaming behavior, bulk density, surface morphology, cell size, compression behavior, dimensional stability, water uptake and thermal stability. It is noted that all the measurements were made in the direction parallel to the foaming rise direction.

2.3. Characterization

The cream time (the time from pouring the isocyanate into the polyol blend until initiation of foaming), end of rise time (the time from pouring the isocyanate into the polyol blend until full expansion of foaming) and tack-free time (the time from pouring the isocyanate into the polyol blend until the skin of the foam was no longer sticky when lightly touched) were recorded during the foaming process.

The foams were cut into squares measuring 25x25x25 mm using a sharp knife. Samples were carefully weighed using an analytical balance with a precision of 0.0001 unit and the dimensions were measured using a digital vernier caliper with a precision of 0.01 unit. The bulk density of the foams in kg/m^3 was simply calculated as a weight/volume ratio. The density of each sample was ascertained using the average value of five specimens.

Samples were frozen at -25ºC, cut into 10x10x5 mm pieces with a sharp knife and coated with gold prior to the morphology study using scanning electron microscopy (SEM), JEOL JSM-6460LV, Japan with an acceleration voltage of 10 kV. The cell size was defined by feret diameter (the longest distance between any two points along the cell boundary in one cell) [20]. The cell sizes were manually measured using SEMAfore image analysis. For each specimen, the average cell size was calculated by averaging several tens of individual cells.

The compressive strength of the foams was tested using a universal testing machine (Instron 4411) equipped with a 500 N load cell. The testing was carried out with a constant crosshead speed of 2.0 mm/min and decompression was done at the same rate when the deformation reached 40% of the original thickness. Then, the foam was recompressed when the crosshead reached the initial position. Four repetitions of the cyclic loading for each sample were carried out. The maximum compressive strength (when the deformation reached 10% at the first cycle) and stress-strain curve behavior for all cyclic curves were evaluated. The specimen dimensions were 50x50x25 mm, the thickness was parallel to foam rising direction, and the samples were conditioned at 20ºC and in 23% RH for 24 h prior the testing. Three samples for each formulation were measured and the average value is reported.

The samples with dimensions of 50x50x25 mm were first conditioned at 25ºC for 24 h before being transferred into controlled temperature at 60ºC and -25ºC, respectively, for 7 days. The dimensional stability as volumetric swelling at 60ºC and volumetric shrinkage at -25ºC were measured, respectively, using the following equation:

$$V_{change}=[(V_2-V_1)/V_1]x100\% \quad (1)$$

where V_1 is the original foam volume before heating or freezing conditioning and V_2 is the final volume after conditioning. The length, width and thickness of the samples were measured using a vernier caliper with 0.01 unit.

The samples with dimensions 20x20x20 mm were immersed in a water bath at ambient temperature, the weight increase of the foams was monitored for various soaking times (from 0.5 h to 5 h). The water uptake was measured according to following equation:

$$W_u=[(m_2-m_1)/m_1]x100\% \quad (2)$$

where m_2 refers to the weight of the sample after immersion and briefly absorbing the excess surface water with soft paper, and m_1 refers to the original weight before the water immersion. Five samples for each type of foam were monitored and the average values were reported.

TGA analysis has been carried out using a TA Instruments TGA analyzer, model Q500 (New Jersey, USA). The temperature range was set from 25ºC to 700ºC with a heating rate of 10ºC/min in an air atmosphere.

3. Results and discussion

3.1. Foaming

Table 2 shows the foaming behavior of BPU foam and BPU nanocomposite foams compared with the reference PPU foam. In general, the cream time and end of rise time can be used to characterize the expansion, whereas the tack-free time can be related to the rate of gelation. Cream time, end of rise time and tack-free time for BPU foam and BPU nanocomposite foams were very similar, indicating that the incorporation of the CNC does not significantly affect foaming behavior. Similar results were obtained by Mosiewicki et al. [8]. However, both the rate of expansion and the gelation of BPU were slower than that of the reference PPU foam. This may be attributed to the secondary hydroxyl groups in the palm oil polyol, resulting in strong steric hindrance. This is also in agreement with previous research results [32]. Moreover, this palm oil polyol displays low hydroxyl values and functionality, while the reference petroleum polyol shows primary hydroxyl groups, high hydroxyl values and functionality. As expected, this difference in functionality and hydroxyl values affects the reactivity. Therefore, it is necessary to balance the reaction between polyol-isocyanate and water-isocyanate in BPU and nanocomposite foams to avoid shrinkage and collapse. Thus the

water was added in the last stage of the process to give sufficient time for the pMDI to react with the polyol before the foaming. Also, the incorporation of CNC with good dispersion is of importance. Therefore, a novel foaming formulation was developed, dry CNC were mixed first with the polyol, and then the blowing agent (water) was added into the foaming process in the last step under vigorous stirring.

3.2. Structure and properties

The prepared foams and their microstructures are shown in Fig. 2. As seen, the PPU foam (Fig. 2a) is yellow and has a large cell size compared to the BPU foam (Fig. 2b). The addition of CNC in BPU (Fig. 2c) resulted in a whiter foam and in a smaller cell size. In Fig. 2d it is evident that the cell walls of the PPU foam were significantly thicker and the cell struts were larger than those of the BPU foam in Fig. 2e and BPU nanocomposite foams in Fig. 2f. No significant difference in the cell wall thickness of BPU foam and BPU4 nanocomposite foam was seen, except that the BPU4 nanocomposite foam (Fig. 2f) has a larger strut area. The larger strut area is expected to improve the mechanical strength of the nanocomposite foam. It is possible that the CNC acts as a nucleating agent in the foaming process, resulting in a larger cell strut area. The cell shape was irregular in all the foams; most of the cells in the BPU foam were oval. However, these cells became more irregular and narrow (higher length/width ratio) after the incorporation of CNC, as illustrated in Fig. 2e and Fig. 2f. This is in agreement with other researchers' results [17,18].

Some interesting features of the foams are illustrated in the Fig. 3, showing that the cell size distribution changed to a narrow range and higher distribution fraction with increased CNC content, resulting in a more uniform foam. The PPU foam had the largest cell size and the widest size distribution. The reason is that the rate of gelation of

the PPU foam is much faster than the rate of expansion, leading to the formation of a skeleton of foam while the CO_2 was being generated. In general, this is attributed to higher reactivity of the petroleum-based polyol.

Fig. 3 show that the average cell size of BBU foam was reduced from 403 to 264 μm with an addition of 1 phr CNC. A possible explanation could be that more carbon dioxide was generated. Hence, smaller cells were produced in the presence of CNC, as evident in Fig. 3. A similar observation was reported in a previous study [18]. In contrast, when the CNC content is increased from 1 to 4 phr, the average cell size of the BPU foams increases from 264 to 303 μm. Presumably CNC acts as nucleation sites to facilitate the cell nucleation process and elongated the cell shape as shown in Fig. 2. This observation is in line with previous observations of larger principal cell diameters with addition of microfibrillated cellulose in biomimetic foams [33].

As seen in the Table 3, all the prepared foams had a bulk density of around 50 kg/m^3. The PPU foam and the nanocomposite foams had slightly higher density of 52 and 53 kg/m^3, respectively.

The compressive strength of the BPU foam increased with the addition of CNC, as seen in the Table 3, reaching the highest value, 117 kPa with 4 phr CNC, which is around two times more than that of the neat BPU foam at 10% deformation and only slightly lower than that of the PPU foam (125 kPa). The compressive strength was reduced when the concentration of the CNC was further increased. The same tendency was observed by Li et al. [21].

The addition of the CNC in the BPU also significantly increases the compressive modulus, as shown in Table 3. The same concentration, 4 phr, increased the modulus from 1021 kPa for the neat BPU foam to 3325 kPa for the nanocomposite BPU4. This is

a three-fold increase. However, the compresive modulus of the PPU foam is still much higher, 9500 kPa.

The improvement in compressive strength and modulus for nanocomposite foams with low concentration of CNC is due to the higher rigidity of the CNC and good dispersion of CNC in the foam mixture, which increases the foam cell wall rigidity. Although this increase tended to decrease with the higher CNC loading (8 phr), which might be because of poor dispersion of the CNC and increased density of the mixture, it was still much higher than neat BPU foam.

The cyclic compression stress-strain curves of the BPU foam, BPU nanocomposite foams and PPU foam are shown in Fig. 4. It is clearly seen that incorporation of CNC significantly increased the rigidity of BPU nanocomposite foams by visual slope extent observation of the cycle 1 curve in the plateau region, while the cycle 1 curve for PPU foam was flat, which means it is an absolutely rigid foam.

In cyclic compression, meanwhile, the extent of strain of the cycle 2 and 3 curves also indicates the rigidity of the foams. In BPU nanocomposite foam preparation, when the amounts of CNC was increased to 4 phr, the extent of strain of cycle 2 has been increased from strain of 10% for BPU foam to 15% for BPU4 nanocomposite foams. This behavior indicates again that the CNC addition improved the rigidity of BPU foams.

The results from compressive testing indicate that there is a strong interaction between the CNC and the PU-matrix which restricts the deformation of the nanocomposite foams. Although the rigidity of the nanocomposite foams was increased, the extent of enhancement was limited. Therefore, BPU nanocomposite foams were considered as semi-rigid bio-polyurethane foams.

In general, there were two ways to improve the mechanical strength of the foam, one was to increase density, another was to reinforce the skeleton structure of the cell strut and cell wall. In this study, this increase was attributed to reinforcement of the cell struts and cell walls, because the density increase was not significant.

3.3. Dimensional stability

Dimensional stability is also an important characteristic of foams used as core material in composite laminates. BPU foam without CNC is inferior to PPU foams for both volumetric shrinkage and swelling, as seen in the Fig. 5, but they were insignificantly different when exposed to aging conditions for 7 days at 60°C and -25°C, respectively.

The results show that both the volumetric swelling and the shrinkage decreased with increasing CNC content, which might depend on the thermodynamic compatibility between the polyurethane and CNC. The volumetric swelling decreased from 13% for the BPU foam to 9% for BPU2 nanocomposite foam, and the shrinkage decreased from 5% to 3%, respectively. When the CNC content was increased to 8 phr, the volumetric swelling and shrinkage were further decreased to 7% and 1%, respectively. Therefore, the addition of CNC significantly improved the dimensional stability of the BPU foams. As expected, the absolute value of volumetric shrinkage at -25°C was significantly lower than the volumetric swelling at 60°C compared to both sides of the x-axis for all the foams. It was concluded that all the foams had better freeze resistance than heat resistance.

3.4. Water uptake

Fig. 6 shows the monitored water uptake, exhibiting a behavior where the water fills the cells very quickly and reaches equilibrium after 1 h for the BPU and BPU

nanocomposite foams, and after 2 h for the PPU foam. At the equilibrium level, the water uptake for PPU foam (436%) was much higher compared to that of the BPU (32%) because of the larger cell size. A slight increase of the water uptake for BPU nanocomposite foams with the addition of CNC is seen; however, this change is not significant, as shown in Fig. 6. The later observation could possible be attributed to differences in cell size, or could be due to the content of closed cells in a composite foams.

3.5. Thermal properties

The thermal stability of the prepared foams is shown in Fig. 7. It can be seen that BPU foams had two stages of degradation and the PPU foam had three stages of degradation during heating. The initial stage of weight loss at 320°C might correspond to bio-polyol component, whereas the second-stage degradation that occurred at around 500°C is mainly due to the isocyanate component of BPU foams. This finding is in agreement with another study by Gu et al. [20]. The degradation temperatures of the BPU decreased slightly with addition of CNC above 220°C. Similar resuts were reported by Gu et al. and Guan et al. [20, 34], who reported that lignocellulosic fibers changed the thermal degradation of PU foam and the incorporation of chitin nanowhiskers decreased the degradation temperature of the PLA/PHBV-Chitin composites, respectively.

4. Conclusions

In this study a bio-polyurethane foam with a density of 50 kg/m^3 was developed and its properties were modified with cellulose nanocrystals (CNC). The addition of CNC was found to influence the cell size, mechanical properties, dimensional stability, water uptake and thermal behavior of the foam.

The cell size, cell distribution and cell shape of the BPU nanocomposite foams were affected in the presence of CNC.

Generally, the addition of CNC in the BPU improved the compression properties of the foam. The best properties were recorded for the nanocomposite foam with 4 phr CNC, where the compressive strength improved from 54 to 117 kPa and the modulus from 1021 to 3225 kPa, compared to the BPU foam. Additionally, the cyclic compressive test indicated that the addition of CNC significantly increased the rigidity, leading to decreased deformation resilience.

The dimensional stability in freezing and heating conditions was shown to be improved with the addition of CNC. This dimensional stability for BPU nanocomposite foams was superior if compared to PPU foam. Freeze resistance is always better than heat resistance for all foams. The water uptake of PPU foam was significantly higher than that of BPU nanocomposite foam. The thermal degradation decreased with increasing CNC content above 220°C.

Acknowledgements

The authors gratefully acknowledge financial support under INCOM EC FP7, Grant Agreement No:608746. PolyGreen in Malaysia and Perstorp in Sweden are gratefully acknowledged for supplying materials. The authors wish to thank Dr. Nicole Stark at USDA Forest Products Laboratory FPL, USA, for kindly providing the cellulose nanocrystals (2013-FPL-CNC-049).

References

[1] Szycher M. Szycher's Handbook of Polyurethanes. Boca Raton, FL: CRC press, New York, 1999.

[2] Yao Y, Yoshioka M, Shiraishi N. Water−absorbing polyurethane foams from liquefied starch. J Appl Polym Sci 1996;60(11):1939-1949.

[3] Abdel Hakim A, Nassar M, Emam A, Sultan M. Preparation and characterization of rigid polyurethane foam prepared from sugar-cane bagasse polyol. Mater Chem Phys 2011;129:301-307.
[4] Seydibeyoğlu MÖ, Misra M, Mohanty A, Blaker JJ, Lee K, Bismarck A, Kazemizadeh M. Green polyurethane nanocomposites from soy polyol and bacterial cellulose. J Mater Sci 2013;48(5):2167-2175.
[5] D'Souza J, Camargo R, Yan N. Polyurethane foams made from liquefied bark‐based polyols. J Appl Polym Sci 2014;131(16) DOI: 10.1002/app.40599.
[6] Guo A, Javni I, Petrovic Z. Rigid polyurethane foams based on soybean oil. J Appl Polym Sci 2000;77(2):467-473.
[7] Gu R, Konar S, Sain M. Preparation and characterization of sustainable polyurethane foams from soybean oils. J Am Oil Chem Soc 2012;89(11):2103-2111.
[8] Mosiewicki M, Dell'Arciprete G, Aranguren M, Marcovich N. Polyurethane foams obtained from castor oil-based polyol and filled with wood flour. J Comp Mater 2009;43(25):3057-3072.
[9] Chian K, Gan L. Development of a rigid polyurethane foam from palm oil. J Appl Polym Sci 1998;68(3):509-515.
[10] Badri K, Othman Z, Ahmad S. Rigid polyurethane foams from oil palm resources. J Mater Sci 2004;39(16):5541-5542.
[11] Lee C, Ooi T, Chuah C, Ahmad S. Rigid polyurethane foam production from palm oil-based epoxidized diethanolamides. J Am Oil Chem Soc 2007; 84(12):1161-1167.
[12] Guo A, Zhang W, Petrovic ZS. Structure–property relationships in polyurethanes derived from soybean oil. J Mater Sci 2006;41(15):4914-4920.
[13] Badri K, Ahmad S, Zakaria S. Development of zero ODP rigid polyurethane foam from RBD palm kernel oil. J Mater Sci Lett 2000;19(15):1355-1356.
[14] Fornasieri M, Alves JW, Muniz EC, Ruvolo-Filho A, Otaguro H, Rubira AF, de Carvalho GM. Synthesis and characterization of polyurethane composites of wood waste and polyols from chemically recycled pet. Comp Part A 2011;42(2):189-195.
[15] Rivera-Armenta J, Heinze T, Mendoza-Martinez A. New polyurethane foams modified with cellulose derivatives. Eur Polym J 2004;40(12):2803-2812.
[16] Seydibeyoğlu Ö M, Oksman K. Novel nanocomposites based on polyurethane and micro fibrillated cellulose. Compos Sci Technol 2008;68(3):908-914.

[17] Silva M, Takahashi J, Chaussy D, Belgacem M, Silva G. Composites of rigid polyurethane foam and cellulose fiber residue. J Appl Polym Sci 2010;117(6):3665-3672.
[18] Zhu M, Bandyopadhyay−Ghosh S, Khazabi M, Cai H, Correa C, Sain M. Reinforcement of soy polyol based rigid polyurethane foams by cellulose microfibers and nanoclays. J Appl Polym Sci 2012;124(6):4702-4710.
[19] Li Y, Ragauskas AJ. Ethanol organosolv lignin-based rigid polyurethane foam reinforced with cellulose nanowhiskers. RSC Adv 2012;2(8):3347-3351.
[20] Gu R, Sain MM, Konar SK. A feasibility study of polyurethane composite foam with added hardwood pulp. Ind Crops Prod 2013;42:273-279.
[21] Li S, Li C, Li C, Yan M, Wu Y, Cao J, He S. Fabrication of nano-crystalline cellulose with phosphoric acid and its full application in a modified polyurethane foam. Polym Degrad Stab 2013;98(9):1940-1944.
[22] Gong G, Pyo J, Mathew AP, Oksman K. Tensile behavior, morphology and viscoelastic analysis of cellulose nanofiber-reinforced (CNF) polyvinyl acetate (PVAc). Comp Part A 2011;42(9):1275-1282.
[23] Mahfuz H, Rangari VK, Islam MS, Jeelani S. Fabrication, synthesis and mechanical characterization of nanoparticles infused polyurethane foams. Comp Part A 2004;35(4):453-460.
[24] Cao X, Dong H, Li CM. New nanocomposite materials reinforced with flax cellulose nanocrystals in waterborne polyurethane. Biomacromol 2007;8(3):899-904.
[25] Lin N, Huang J, Chang PR, Feng J, Yu J. Surface acetylation of cellulose nanocrystal and its reinforcing function in poly (lactic acid). Carbohydr Polym 2011;83(4):1834-1842.
[26] Mathew AP, Oksman K, Karim Z, Liu P, Khan SA, Naseri N. Process scale up and characterization of wood cellulose nanocrystals hydrolysed using bioethanol pilot plant. Ind Crop Prod 2014;58:212-219.
[27] Uddin AJ, Araki J, Gotoh Y. Characterization of the poly(vinyl alcohol)/cellulose whisker gel spun fibers. Comp Part A 2011;42:741-747
[28] Bondeson D, Oksman K. Polylactic acid/cellulose whisker nanocomposites modified by polyvinyl alcohol. Comp Part A 2007;38(12):2486-2492.

[29] Visakh P, Thomas S, Oksman K, Mathew AP. Crosslinked natural rubber nanocomposites reinforced with cellulose whiskers isolated from bamboo waste: Processing and mechanical/ thermal properties. Comp Part A 2012;43(4):735-741.
[30] Auad ML, Mosiewicki MA, Richardson T, Aranguren MI, Marcovich NE. Nanocompo-sites made from cellulose nanocrystals and tailored segmented polyurethanes. J Appl Polym Sci 2010;115(2):1215-1225.
[31] Faruk O, Sain M, Farnood R, Pan Y, Xiao H. Development of Lignin and Nanocellulose Enhanced Bio PU Foams for Automotive Parts. J Polym Environ 2014;22(3):279-288.
[32] Hu YH, Gao Y, Wang DN, Hu CP, Zu S, Vanoverloop L, Randall D. Rigid polyurethane foam prepared from a rape seed oil based polyol. J Appl Polym Sci 2002;84(3):591-597.
[33] Svagan AJ, Samir MA, Berglund LA. Biomimetic foams of high mechanical performance based on nanostructured cell walls reinforced by native cellulose nanofibrils. Adv Mater 2008;20(7):1263-1269.
[34] Guan Q, Naguib HE. Fabrication and Characterization of PLA/PHBV-Chitin Nanocomposites and Their Foams. J Polym Environ 2014;22(1):119-130.

Figure Captions

Fig. 1. Schematic diagram of the lab-scale foaming process of BPU foam and nanocomposite foams.

Fig. 2. Cell morphology and appreance of prepared foams (a) PPU, (b) BPU, (c) BPU4 nanocomposite and detailed views showing cell wall and strut area of (d) PPU, (e) BPU and (f) BPU4 nanocomposite.

Fig. 3. Cell size distribution of BPU foam with different CNC contents compared with PPU foam.

Fig. 4. Stress-strain curves in cyclic loading of the semi-rigid BPU foam with different CNC contents compared with PPU foam.

Fig. 5. Dimensional stability of neat BPU foam, BPU nanocomposite foams with CNC and PPU foam at freezing and heating condition.

Fig. 6. Water uptake of the prepared pure BPU foam and BPU nanocomposite foams with CNC compared with pure PPU foam.

Fig. 7. Thermal properties of BPU nanocomposite foams with or without CNC compared with PPU foam.

Table captions

Table 1. Foaming formulation for semi-rigid BPU nanocomposite foams and PPU foam.

Table 2. Foaming behavior of the BPU foam, BPU nanocomposite foams and PPU foam.

Table 3. Effect of CNC contents for BPU nanocomposite foams on bulk density, compressive strength, compressive modulus and water uptake at equilibrium level.

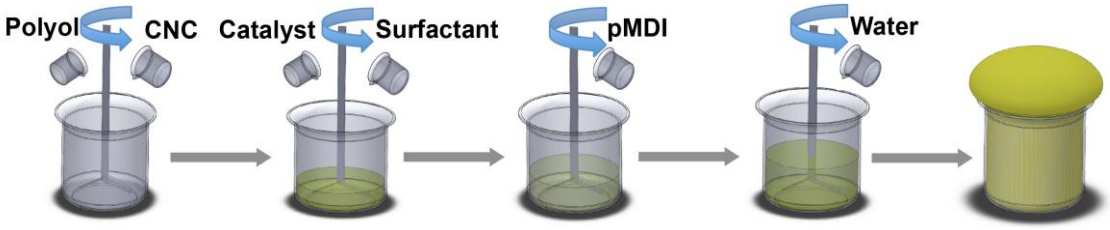
Polyol
CNC
Catalyst
Surfactant
pMDI
Water

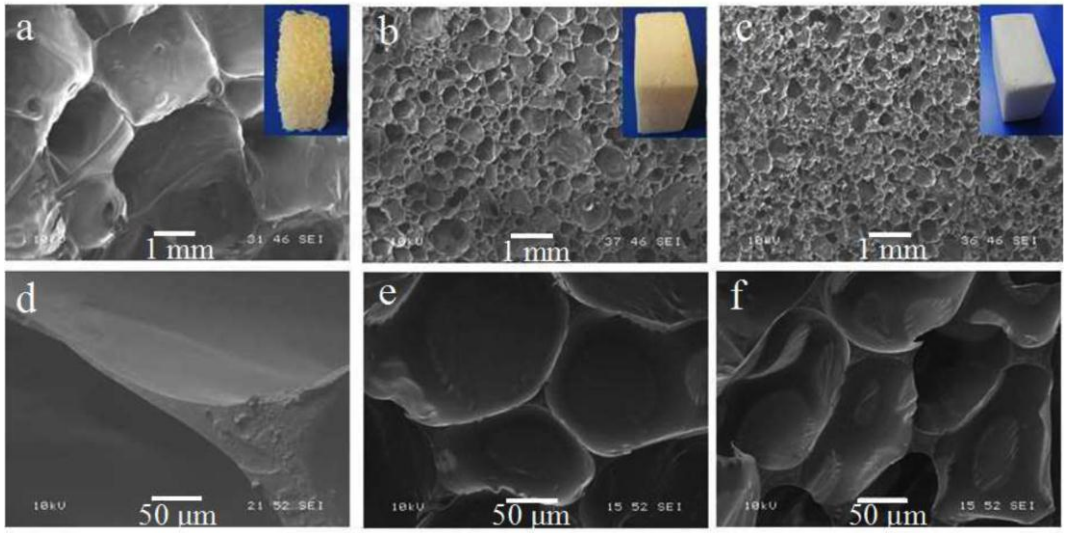
a
1 mm
b
1 mm
c
1 mm
d
50 µm
e
50 µm
f
50 µm

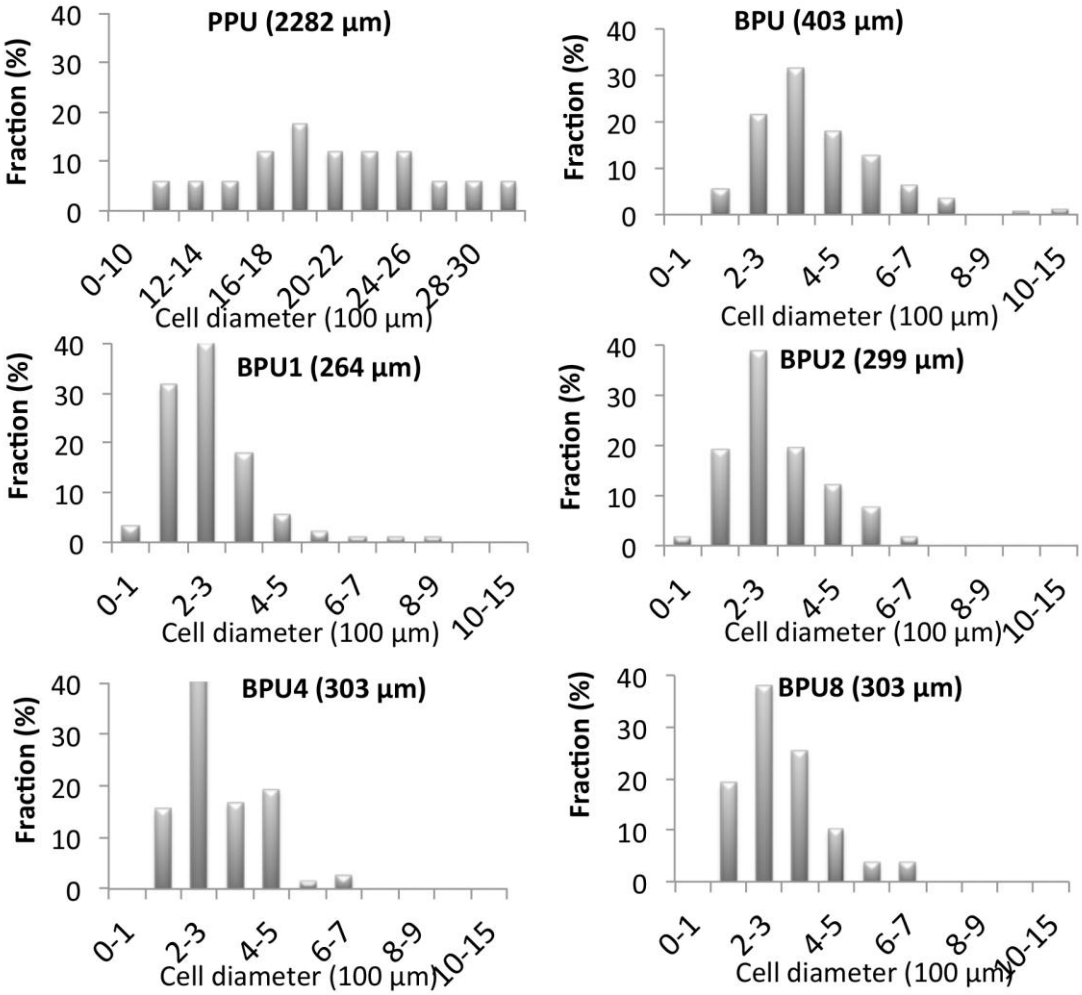
PPU (2282 µm)
BPU (403 µm)
BPU1 (264 µm)
BPU2 (299 µm)
BPU4 (303 µm)
BPU8 (303 µm)
Fraction (%)
Cell diameter (100 µm)
0-10
12-14
16-18
20-22
24-26
28-30
0-1
2-3
4-5
6-7
8-9
10-15

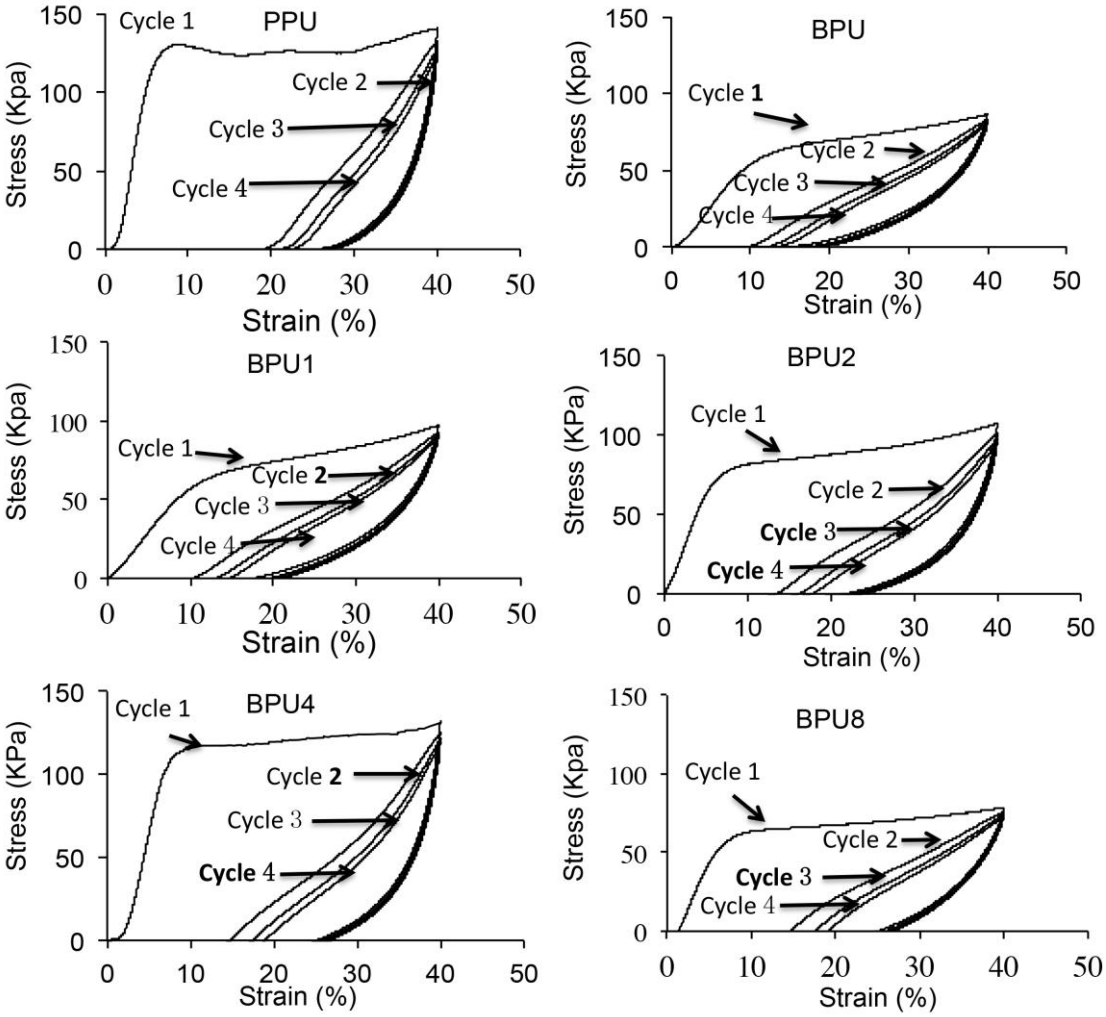
PPU
Cycle 1
Cycle 2
Cycle 3
Cycle 4
Stress (Kpa)
Strain (%)
BPU
Cycle 1
Cycle 2
Cycle 3
Cycle 4
Stress (Kpa)
Strain (%)
BPU1
Cycle 1
Cycle 2
Cycle 3
Cycle 4
Stess (Kpa)
Strain (%)
BPU2
Cycle 1
Cycle 2
Cycle 3
Cycle 4
Stress (KPa)
Strain (%)
BPU4
Cycle 1
Cycle 2
Cycle 3
Cycle 4
Stress (KPa)
Strain (%)
BPU8
Cycle 1
Cycle 2
Cycle 3
Cycle 4
Stress (Kpa)
Strain (%)

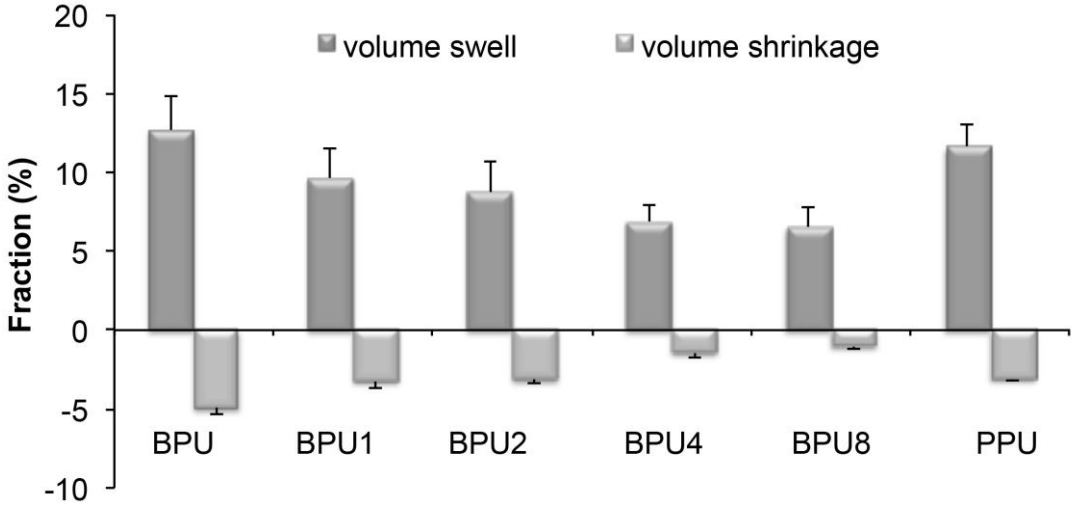
20
15
10
5
0
-5
-10
Fraction (%)
volume swell
volume shrinkage
BPU
BPU1
BPU2
BPU4
BPU8
PPU

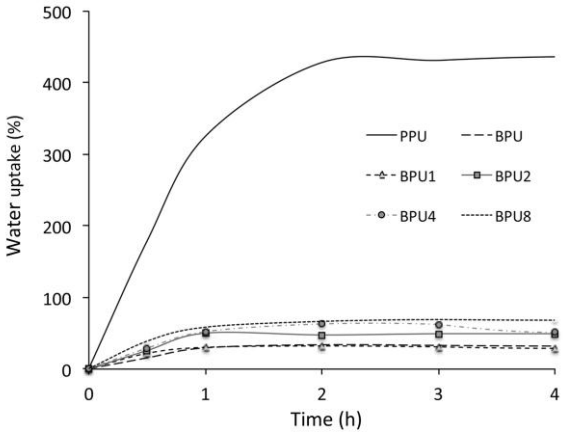
500
400
300
200
100
0
Water uptake (%)
0
1
2
3
4
Time (h)
PPU
BPU
BPU1
BPU2
BPU4
BPU8

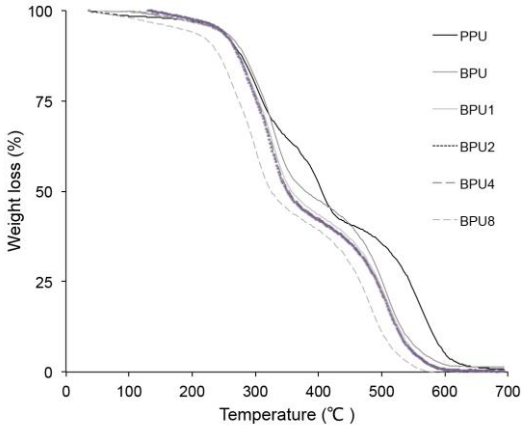
100
75
50
25
0
Weight loss (%)
0
100
200
300
400
500
600
700
Temperature (℃)
PPU
BPU
BPU1
BPU2
BPU4
BPU8

Table 1. Foaming formulation for semi-rigid BPU nanocomposite foams and PPU foam

Components	Parts of component (phr)	Role
Polyol	100	Base of resin
pMDI	126 (150 $_{PPU}$)	Reactive prepolymer
Triethylamine	2	
Dibutyltin dilaurate	2.6	
Polydimethyl siloxane	5	Surfactant
Silicone oil	5	
Water	4	Blowing agent
CNC	1, 2, 4, 8	Reinforcement
Index (-NCO/-OH)	1.5	Both materials

Table 2. Foaming behavior of the BPU foam, BPU nanocomposite foams and PPU foam

Foams	Cream time (s)	End of rise time (s)	Tack free time (s)
BPU	13	37	85
BPU1	13	36	86
BPU2	12	38	85
BPU4	14	37	83
BPU8	13	38	86
PPU	10	35	60

Table 3. Effect of different CNC content for BPU nanocomposite foams on bulk density, compressive strength, compressive modulus and water uptake at equilibrium level

Foams	Density (kg/m^3)	Compressive strength (kPa)	Compressive modulus (kPa)	Water uptake (%)
BPU	50 ± 1	54 ± 1	1021 ± 13	32 ± 1
BPU1	50 ± 1	58 ± 1	1025 ± 13	29 ± 1
BPU2	52 ± 1	82 ± 1	2307 ± 10	49 ± 2
BPU4	53 ± 1	117 ± 1	3225 ± 17	51 ± 1
BPU8	53 ± 1	66 ± 2	2037 ± 12	68 ± 2
PPU	52 ± 1	125 ± 1	9501 ± 11	436 ± 5